2018

Energy and thermal performance evaluation of an electrified snow removal system at airports using numerical modeling and field measurements

S.M. Sajed Sadati
Iowa State University

Energy and thermal performance evaluation of an electrified snow removal system at airports using numerical modeling and field measurements

by

SeyedMohammad Sajed Sadati

A thesis submitted to the graduate faculty

in partial fulfillment of the requirements for the degree of

MASTER OF SCIENCE

Major: Civil Engineering (Construction Engineering and Management)

Program of Study Committee:
Kristen Cetin, Co-major Professor
Halil Ceylan, Co-major Professor
David Jeong

The student author, whose presentation of the scholarship herein was approved by the program of study committee, is solely responsible for the content of this thesis. The Graduate College will ensure this thesis is globally accessible and will not permit alterations after a degree is conferred.

Iowa State University

Ames, Iowa

2018

TABLE OF CONTENTS

LIST OF FIGURES

LIST OF TABLES

ACKNOWLEDGMENTS

I would like to thank my advisors, Dr. Kristen Cetin and Dr. Halil Ceylan, who supported me throughout this study. I would also like to thank Dr. Sunghwan Kim for helping me with understanding the project background.

This research was conducted under the Federal Aviation Administration (FAA) Air Transportation Center of Excellence Cooperative Agreement 12-C-GA-ISU for the Partnership to Enhance General Aviation Safety, Accessibility and Sustainability (PEGASAS). I would like to thank the current project Technical Monitor, Mr. Benjamin J. Mahaffay, and the former project Technical Monitors, Mr. Jeffrey S. Gagnon (interim), Mr. Donald Barbagallo, and Dr. Charles A. Ishee for their invaluable guidance during this study. I also would like to thank PEGASAS Industry Advisory Board members for their valuable support and feedback. I would like to thank Mr. Bryan Belt, Director of Engineering at Des Moines International Airport, for his supports throughout this project. Although the FAA has sponsored this project, it neither endorses nor rejects the findings of this research. The presentation of this information is in the interest of invoking comments by the technical community on the results and conclusions of the research.

ABSTRACT

Airports are moving toward the utilization of clean energy technologies along with the implementation of practices that reduce local sources of pollution. This includes replacing fossil fuel-based with electricity-based equipment, technologies, and operations. However, given the anticipated energy demands needed for airport operations electrification, it is important to study airport energy demand profile changes after implementing such systems. Electrically-conductive concrete (ECON) is currently a focus of heated pavement design for replacing conventional practices of removing snow and ice. ECON heated pavement systems (HPSs) use electricity to heat the surface of the pavement. Since experimental studies are resource intensive and the performance of ECON HPS depends on weather conditions, developing a field data-validated numerical model enables the evaluation of its long term energy costs. In this research, a finite element (FE) model is developed and experimentally-validated using two proposed model-updating methods for full-scale ECON HPS test slabs constructed at Des Moines International Airport (DSM), Iowa. The modeling methods are able to predict energy demands and average surface temperatures within 2% and 13% respectively, across a range of snowfall rates and weather conditions. This validated model is then used to evaluate the energy consumption and thermal performance of ECON HPS at DSM, using weather conditions during typical snow events derived from typical meteorological year (TMY) data as model inputs. The estimated power demand ranges from 325 to 460 W/m^2 for different weather conditions; the monthly consumption is the highest in a typical January, ranging from 165 to 446 MWh for the smallest and largest typical airport terminal gate sizes. The results of this study demonstrate the accuracy benefits of the use of model updating methods, and provide a validated tool

that can be used to evaluate the energy demand of ECON HPS and develop control strategies for minimizing the demand in a diversity of weather scenarios and locations.

CHAPTER 1. INTRODUCTION

Transportation infrastructure, including airports, is moving toward the use of clean energy technologies and reducing the need for conventional practices that create local sources of pollution and have high environmental impacts [1–3]. This includes replacing fossil fuel-based with electricity-based operations and equipment [4]. However, given the significant energy demands associated with existing fossil fuel-based operations, the electric power demand of alternative electric systems must be assessed to evaluate the technical feasibility of electrifying such operations and equipment. Among the electric systems that could replace conventional practices at an airport, the focus of this research is on electrically-conductive concrete (ECON) heated pavement systems (HPSs) [5].

Snow and ice removal is a necessary effort at many airports, particularly those located in cold regions with frequent and periodic snow and ice events during the winter season. Current methods for snow and ice removal commonly use fossil fuel-powered vehicles and snow plowing equipment, or melt snow and ice using chemicals [6,7]. During snow removal operations, snow is typically plowed into piles in designated areas [8]. At many airports the piles of plowed snow may also be melted using either stationary or mobile snow-melting equipment. Not only do such conventional methods have high environmental and air quality impacts, they are also time-consuming for airport personnel and can be costly, sometimes resulting in delays and airplane accidents at the airports [9,10]. Snow and ice removal can also be challenging, particularly from the apron areas of airports where there is significant equipment, movement of both people and vehicles, traffic, and related congestion [8]. For this particular type of area, snow and ice can also represent a safety hazard for both passengers and airport workers. Moreover, when chemicals are used for snow and ice removal, the lifetime of

the pavement is usually reduced [11,12], resulting in higher maintenance and rehabilitation costs over the pavement's lifetime. Runoff containing such chemicals produce negative environmental consequences [6,13], so there is a growing research focus on alternative snow and ice removal methods, including heated pavement systems [14].

Several recent studies have been conducted on heated pavement systems [15–17]. There are four types of heated pavement systems, including: i) infrared heating [18], ii) electrical heaters embedded in pavement [19], iii) hydronic heating circulating hot water through pipes embedded in pavement [20,21], and iv) electrically conductive concrete and asphalt [22–24]. Electrically-conductive concrete (ECON) heated pavement systems (HPS), the most recently developed among these technologies, are produced by adding electrically conductive material, such as steel shavings [24] or carbon fibers [25] to the concrete mix. The addition of these materials enables the pavement system to act as a resistor, which generates heat when a voltage is applied.

ECON HPS require an external source of electricity to generate and dissipate heat that increases the surface temperature of the pavement sufficiently to melt snow and ice. Therefore, the use of ECON HPS will change the profile of electricity demand of an airport during snow and ice events, particularly if it is widely implemented. Given the move toward dynamic and time-of-use pricing by utilities [26,27], as well as the demand charge-dominant rate structures used today, particularly for commercial facilities, a comprehensive understanding of the performance and associated power demands and energy consumption of such systems is needed. This is more significant considering that the energy management of airports is turning into a challenge given the significant growth of those transportation hubs close to the large cities [3].

To have an accurate estimation of energy consumption of ECON HPS, it is also necessary to study the thermal performance of this system since the goal of implementing ECON HPS is to use electricity to modulate the pavement surface temperature and melt the snow and ice. ECON HPS's thermal performance depends on many factors, and an important factor is boundary conditions, including climatic conditions, to which the ECON HPS is exposed. Since conducting experimental research to determine thermal performance over a wide range of climatic conditions is costly, the availability of a reliable, validated numerical model for assessing system response under different conditions would be beneficial. A second important factor to be considered is the study of system design parameters, including dimensions, layering structure, and thermal properties of the ECON material. The field study of a large number of variations in system properties would be much more costly than using a validated model.

1.1 Literature Review

Much of the existing literature on modeling the thermal performance of concrete focuses on the modeling of portland cement concrete (PCC) not containing electrically conductive materials. Thelandersson [28] modeled the combined effects of structural and thermal loads on concrete using coupled equations describing structural and thermal strains. Thermal strain is considered to be a function of concrete temperature and stress level applied by structural loads and a simplified method for estimating the thermomechanical response of concrete to thermal and structural loads was developed and verified by experimental testing. Huang, et al. [29] developed a nonlinear finite element model for predicting the temperature of reinforced concrete exposed to fire. In that two-dimensional model, one-dimensional heat transfer from fire to the concrete structure was assumed. The model predicts the temperature

increase at different points in the concrete using thermal conductivity and heat capacity matrixes. Nonlinearity of the model was assumed in describing heat transfer between simulated fire and concrete layer, and the reinforcing steel bars were assumed to be in perfect contact with the concrete layer. The developed model was verified by experimental test results.

In another study on material properties of concrete, Khan [30] investigated the significant parameters affecting thermal properties of concrete and models for predicting such properties. In Khan's study, the effect of each component of concrete was investigated and Campbell-Allen and Thorn's model [31] was used to predict the thermal conductivity of a concrete sample based on thermal properties of its components. The results of the model for thermal conductivity came closer to the measured results as the moisture content of the concrete increased. For saturated concrete samples, the thermal conductivity could be estimated with an average error of approximately 10%; for dry samples, the thermal conductivity was overestimated by 22% on average. Thermo-physical properties of concrete were also studied by Shin, et a. [32] and Kodur and Sultan [33]. In both studies, thermal properties of concrete, including thermal conductivity and heat capacity, were studied for temperatures ranging from 20 to 1,000 ˚C. In this research, temperatures between -20 ˚C and 30 ˚C for concrete material are of interest. Considering this range of temperatures, the results of Shin and Kodur's studies show that changes in thermal conductivity and heat capacity are not significant for temperatures between 0 ˚C and 30 ˚C; however, for temperatures below 0 ˚C, these properties require further study.

Focusing on heat dissipation from concrete building floors, Zhong and Braun [34] developed a simplified model with three nodes to study transient heat transfer between concrete slabs and subgrade to estimate heat loss from the floor. A finite element model was used to

verify the results of this model and confirm its accuracy, and reported that the results for several construction configurations, including various edge insulations and soil properties, compared well with the finite element model predications. In another study, Selvam and Castro [35] developed a 3D finite element model for estimating heat transfer in concrete to seek improvement in its properties for energy storage applications. While this model was used to identify parameters that would improve the performance of concrete in terms of storing thermal energy, these studies have not considered ECON. To study the operational strategy of hydronic systems, Xu and Tan [36] utilized a heat and mass-coupled model previously presented by Liu, et al. [37] for performance evaluation of a hydronic system under various weather conditions. The model was used to identify the sensitivity of the energy consumption of a hydronic system to climatic and system parameters. Based on the results of the study by Xu and Tan, ambient temperature (^{o}C) and snowfall rate (mm/hr) are two climatic parameters that most significantly impact the energetic performance of a hydronic system in snow-melting processes, and the heat load applied to the liquid running through the hydronic pipes is another important parameter.

Although there are several experimental studies on ECON HPS [16,38], there are only two previously-known studies on numerical modeling of this type of concrete [24,25], and these studies did not consider heat transfer between all pavement layers. Moreover, there are no previous studies on the energy consumption of these systems. Tuan, et al. [24], primarily studied the experimental performance of ECON material produced using steel shavings. A simplified finite element (FE) ECON model was also developed to predict the temperature increase in an ECON layer due to application of a voltage, although the correspondence of the predicted temperature values with experimentally-measured values was not reported. In the

second study, Abdualla, et al. [25] developed an FE model of a single ECON layer on top of a regular PCC layer, but did not consider other layers of a pavement system. The ECON material was produced by adding carbon fibers to the concrete mix. Abdulla et al., reported that the temperature values predicted at the middle of the ECON surface by the model were consistent with the laboratory experimental temperature measurements. The experimental tests were conducted over 2.5 hours without snow on the surface of the slab, with an initial starting temperature of -1 ˚C. Surface temperature values were not evaluated at other surface and sub-surface locations and the validation of studied models was limited to laboratory experimental cases that did not include modeling the heat loss from the surface due to melting snow and ice. In previous studies on the modeling of ECON, only the top conductive layer has been investigated even though system performance is also dependent on the heat transfer to the layers below. In addition, in previous studies, energy consumption and power demand of the ECON HPS, important factors in the operation of these systems, were not evaluated.

Given the non-uniform heating of the ECON layer associated with dispersion of the carbon fibers, along with other complexities of the ECON material, a more comprehensive understanding is needed to better characterize the overall performance of ECON, including the associated electricity demand and consumption. This would include modeling of all the pavement layers to produce a more detailed understanding of ECON HPS performance in a physics-based model that can, through validation and model-updating, help predict pavement performance under a variety of conditions in terms of melting snow and ice.

1.2 Objectives

The main objective of this research is to develop a field data-validated numerical model of ECON HPS capable of predicting its energy demands and temperature variations at multiple

surface and sub-surface locations of all pavement layers. This model is developed using actual climatic condition data and system parameters, including material properties and the applied voltage using data obtained from ECON HPS test slabs at the Des Moines International Airport (DSM). Based on this numerical model, the power demand of ECON HPS and resultant effect on the energy consumption of an airport are predicted considering typical weather data for the studied airport location. Although the presented methodology is used to evaluate energy performance of the system at DSM, it can be implemented for any location with available weather data. The results of this work are beneficial for providing guidelines for the design of ECON HPS in different climatic zones since the design parameters are highly sensitive to climatic conditions. The effect of implementing ECON HPS on power demand is also an important factor for decision makers who are interested in the feasibility of such systems and comparing them with other snow and ice removal methods. In this respect, having a reliable numerical model that is able to predict the added power demand associated with the use of ECON HPS would be a beneficial tool for developing control strategies to minimize the energy demand.

1.3 Thesis Organization

The remainder of this work is divided into three main sections. Chapter 2 describes the methodology of collecting the data from test slabs, developing the model, and control strategy for operating the model. The model validation and results of energy and thermal performance of the system by applying the proposed control strategy are presented in Chapter 3 as the Results and Discussions. Chapter 4 includes the conclusions of this research and suggestions for future studies.

CHAPTER 2. METHODOLOGY

This section is organized into four subsections. The first subsection summarizes the field implementation of ECON, which is used as the basis of the developed FE model, including the testing of thermal properties during field testing. The second subsection then covers the development of the finite element model, followed by the third subsection which is a description of the model-updating methods. The fourth subsection contains the description of weather conditions energy evaluation method, system size and control strategy.

2.1 ECON Field Testing

2.1.1 ECON Material

The ECON material was prepared using chopped carbon fibers as an electrically conductive additive. Carbon fiber at a dosage of 1% by total volume of concrete mixture, a value based on the results of previous studies, [5,39–43] was used. The chopped carbon fiber is Polyacrilonitrile-based with 95% carbon content and an electrical resistivity of 1.55×10^{-3} Ω-cm [39]. The carbon fiber fraction of the ECON material mixture, 1% of total volume of ECON, is comprised of 70% 6 mm-long fibers and 30% 3 mm-long fibers.

The ECON mix design [44], materials, and hardened properties conform to standard FAA specifications [45,46]. For the test slabs at DSM, 5 m^3 of ECON material was produced in a drum mixer. Carbon fibers in the required amount were dried in an oven at 115˚C for 24 hours, then packed in water-soluble bags to prevent fiber loss during transportation and handling and to expedite the process of feeding the fibers into the mixer.

2.1.2 Slab Construction and Instrumentation

To have an estimation of the heating performance of ECON material a test slab was built in the laboratory consisting of two layers of ECON and PCC. After performing a substantial amount of tests in the laboratory, a full-scale ECON system test slab was constructed at DSM, Iowa [47]. The slab includes a 9 cm ECON layer poured over a 10 cm thick conventional concrete slab with a subbase layer of 20 cm underneath, as shown in Figure 1. The ECON HPS consisted of 3.8 m by 4.6 m slabs with six embedded stainless steel L-shaped electrodes spaced 1 m apart. The electrodes were connected to an external source of electricity to provide a voltage of approximately 210 V. Figure 2 is a thermal image of the ECON HPS surface during one of the test events at an average ambient temperature of 0°C and an average wind speed of 4.1 m/s measured at a height of 10 m.

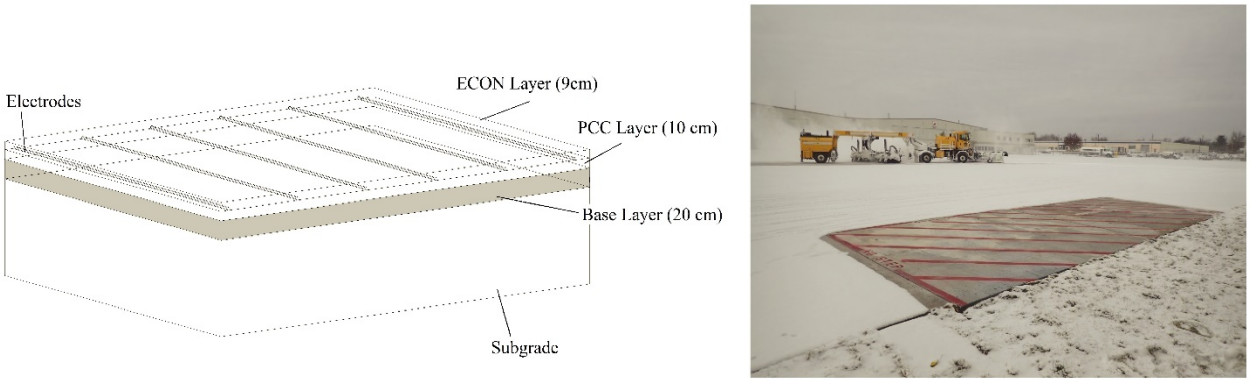

Figure 1. ECON HPS slabs constructed at the Des Moines International Airport in Iowa, including (a) diagram of the layout and layers, and (b) photograph of the field test setup operating in snow conditions [48]

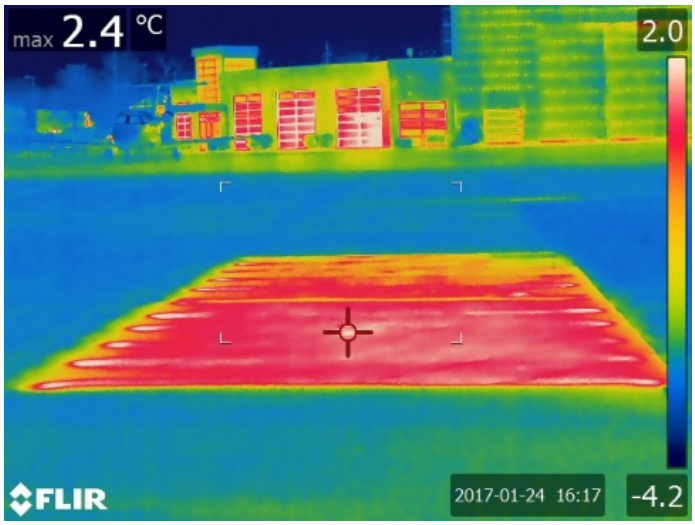

Figure 2. Thermal image of the ECON HPS slabs at DSM during an experimental test under an average ambient temperature of 0 °C and average wind speed of 4.1 m/s measured at a height of 10 m

2.1.3 Field Data Collection and Quality Control

The field test slabs were implemented with temperature sensors embedded at strategic locations (Figure 2) to provide an improved understanding of thermal performance. The temperature sensors consisted of wireless sensors (+/- 1%) [49] and thermistors in installed strain gauge sensors (+/- 0.5 ˚C) [50]. These strain gauges were embedded inside the ECON layer approximately 6 cm from the surface of the pavement, and the wireless sensors were embedded inside each layer of the ECON HPS in the locations shown in Figure 3. The collected field data was quality controlled by checking for sensors and/or periods of time producing noisy data, and for data above or below acceptable temperature thresholds. In order to measure the power demand of the system, voltmeter (+/- 3%) and ammeter (+/- 1%) sensors [49] were used on the main circuit connected to the ECON HPS test slabs. Since electric power is the product of voltage and the current values, the total error was calculated using multiplication error propagation based on the individual errors of each sensor [51]. Table 1 contains the error values for aforementioned sensors.

Table 1. Error ranges for the sensor readings

Parameter	Error
Temperature by wireless temperature sensors	+/- 1%
Temperature by thermistors in strain gauges	+/- 0.5 ˚C
Voltage by voltmeters	+/- 3%
Current by ammeter	+/- 1%
Electric Power (calculated)[1]	$Power \times \sqrt{\left(\frac{Voltage\ Error}{Voltage}\right)^2 + \left(\frac{Current\ Error}{Current}\right)^2}$

[1]*Calculated based on equations in* [51]

The weather data, including ambient temperature and wind speed, were obtained from the US National Centers for Environmental Information [52]. The weather station at DSM is a Class I station, meeting the highest quality standards for weather stations [53]. Performance data used for model construction and validation in this research, including dates, weather conditions, and snowfall rates and amounts, are summarized in Table 2.

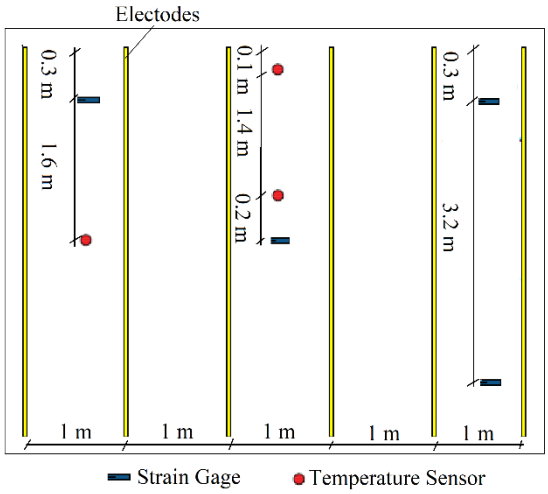

Figure 3. Diagram of sensor layout for one test slab for field data collection used for finite element model validation

Table 2. Des Moines International Airport field test data summary

Purpose	Operation time (hr)	Avg. Air Temp. (°C)	Avg. Wind Speed (m/s)	Avg. Snow Thickness (mm)	Avg. Power Density (W/m^2)	Total Electricity Use (kWh/m^2)
Experimental Test 1: Evaluation of FE model with updating (10 December 2016)	6	-5	5.8	30	414	2.89
Experimental Test 2: Evaluation of FE model using out-of-sample data (9 December 2016)	2.5	-10	10	12.7	408	0.61

2.1.4 Thermal Properties of ECON HPS Field Test Slab

The physical and thermal properties of the test slabs, including the ECON layer, the conventional concrete layer, the stainless steel electrodes, and the subgrade, are summarized in Table 3. The material properties required for input into the FE model include density (kg/m^3), heat capacity (J/kg.°C), thermal conductivity (W/m°C), and electrical resistivity (Ω-cm) of each layer.

Thermal conductivity was assessed using a non-contact, non-destructive technique involving a thermal camera and a laser heating element. A focused laser beam was used as a heating element to heat up a chosen area of a bulk sample of the field-implemented ECON. The temperature rise due to the laser beam was used to plot a chart of results of data from materials with known thermal conductivity to determine the thermal conductivity of the field test ECON section. The specific heat capacity was determined by placing the ECON specimen in a foam box filled with water, and using a heat balance equation and measurements of water and concrete temperatures before and after immersion. The electrical resistivity was determined by measuring current and voltage from the constructed slabs at different temperatures. Concrete density is measured using samples taken from the concrete layers at

DSM during pavement construction. The material properties of the stainless steel electrodes and the subgrade are taken from data available in the literature, including [54] and [55], respectively.

Table 3. Material properties of test slab used for the developed finite element model

Material Type	ECON Slab[1]	Conventional Concrete Layer	Stainless Steel Electrodes[2]	Base Layer[3]	Subgrade[3]
Density (kg/m^3)	2,500	2,300	7,800	1,500	1,500
Heat Capacity (J/kg.˚C)	1300	880	475	840	800
Thermal Conductivity (W/m˚C)	1.35	1.4	44	1.3	1
Electrical Resistivity (Ω-cm)	900	5.4×10^5	1.7×10^{-9}	5×10^5	1.5×10^4

[1] *Electrical resistivity, heat capacity and thermal conductivity of ECON slab measured at 22 ˚C*
[2] *Steel properties utilized are based on* [56]
[3] *Subgrade properties utilized are based on* [54]

2.2 Finite element model of ECON

The ECON HPS finite element (FE) model, capable of reflecting electrical, thermal, and structural loads and responses, is produced using ANSYS 18.2 [57]. ANSYS is commonly used and well-known in the field of thermoelectric FE modeling. A model of a laboratory test slab was built and the results were compared with the temperature measurements from that slab prior to the developing the model of the full scale slab at DSM. To model the thermal performance of the ECON HPS constructed at DSM, transient thermal analysis is used. The elements used for the modeling are the SOLID5 element type for the ECON, PCC, base, and subgrade layers, and the PLANE13 element type for the stainless steel electrodes placed within the body of ECON layer. Since SOLID5 and PLANE13 are capable of handling the electrical, thermal, and structural loads and responses required for the ECON HPS model, more complex element types are not required. These element types are also compatible and can be integrated and used in the same model. There are 9,562 elements in the model, including smaller elements where the mesh size is made finer in and around the electrodes because of their higher aspect

ratio. The average size of the elements is approximately 10×10×10 cm^3 for subgrade and as small as 2×2×2 cm^3 for elements close to the electrodes. The meshed model and the elements are shown in Figure 4. The element sizes were found by running the model with the same set of inputs while varying the mesh size and then comparing the results. The change in temperature results was less than 0.5% for element sizes smaller than the selected size which can be considered negligible for the estimations in this research [58]. A full transient solution with time-steps of 5 minutes was sought because this time-step increment provides a sufficient number of data points for post-processing purposes and is small enough to produce an accurate solution, as checked by running the model using a range of different time-steps.

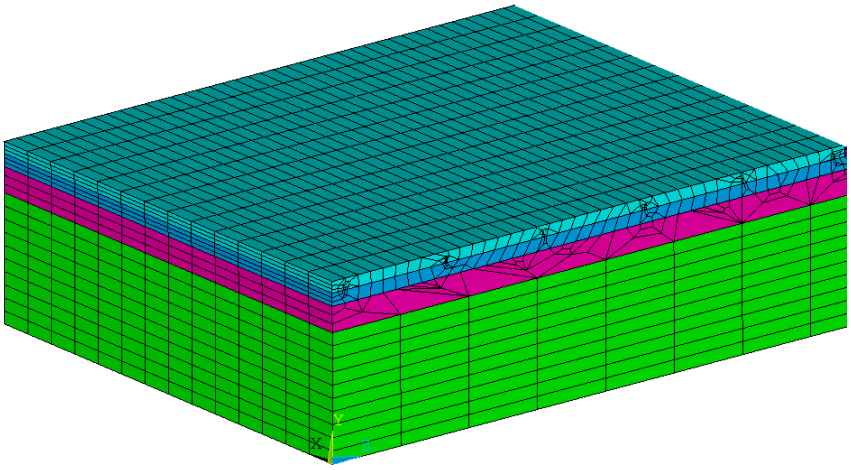

Figure 4. Elements of the finite element model of ECON system

The material properties corresponding to the ECON, PCC, base, and subgrade layers, including the density, heat capacity, thermal conductivity and electrical resistivity values given in Table 3, were assigned to the elements. Heat conduction is assumed to occur between the model layers. Heat loss from the top surface of the ECON layer is modeled as a convection load based on wind speed, because the top surface is assumed to be exposed to outdoor ambient temperature conditions. Zero solar radiation is assumed in this model because the modeling of the slab performance was either for cloudy conditions with minimal diffuse solar radiation

reaching the pavement surface, or during evening or night hours where there is no solar radiation. The results from this model are thus applicable only for conditions where there are no significant solar loads, which is likely to be the case during significant snow events. The vertical sides of the slabs are considered to exhibit negligible heat transfer with surrounding concrete slabs compared to the heat loss from the top surface, an assumption consistent with the modeling methods described in previous literature [25]. Therefore, except for the top surface and heat transfer between interlayers, the other sides of the model are considered to be adiabatic. A voltage is applied to each pair of electrodes and the model's heat generation and heat transfer behavior are studied and compared with measured temperature values.

2.3 Model-updating method for finite element model

To further improve the model results, updating the model was performed to improve the matching of the model results to real-world performance. This process is also called calibration in some fields [59]. These resulting modifications involved making slight changes typically in the material properties of the elements used in the model. In this case of a FE model of ECON, the resistivity of concrete depends on its temperature [60], so the resistivity values of ECON layer samples measured at room temperature (22 ˚C) may not reflect the actual resistivity of the ECON material in the field. The differences between measured resistivity values of samples and the resistivity values of ECON in the full-scale slab are introduced into the FE model using a model-updating method. As a scientific basis for such model-updating, two different parameters are considered: i) temperature of ECON layer, and ii) power demand of ECON HPS. The first is based on the temperatures measured at several points of the ECON layer, while the second is based on the power that could be drawn by the ECON layer. The advantage of considering the second parameter over the first is that it includes the contribution

of the whole body of the ECON layer while the first parameter includes temperatures at a few points where the sensors are embedded inside the ECON layer. Making a choice between these two options depends on the modeling objectives, i.e., either estimating the performance of the system in terms of temperature increase, or estimating the electricity use. These two model-updating methods are explained in the following subsections.

2.3.1 Model-updating Based on Measured Temperature Values

This method uses equations reflective of the conversion of electrical energy to thermal energy and the resulting change in ECON temperature. Eq. (1) calculates the power converted to thermal energy,

$$P = RI^2 \tag{1}$$

where P is the power, R is the resistance of the material, and I is the electrical current flowing in ECON due to the voltage between each electrode pair. R can be calculated using resistivity (ρ) using Eq. (2) [61],

$$R = \frac{\rho L}{A} \tag{2}$$

where, L and A are the length and cross-sectional area of the ECON in the direction of electrical current flow. I can be calculated from the current density (J) by multiplying the electrical conductivity (σ) by electric field (E) as shown in Eqs. (3) and (4) [61].

$$\mathrm{J} = \sigma \mathrm{E} \tag{3}$$

$$|\mathrm{J}| = \frac{I}{A} \tag{4}$$

Temperature increase and thermal energy accumulated inside the slabs can be related using Eq. (5),

$$\frac{dQ}{dt} = mC\frac{\Delta T}{dt} \tag{5}$$

where $\frac{dQ}{dt}$ is the rate of change in thermal energy, m is mass, C is the specific heat capacity, and $\frac{\Delta T}{dt}$ is the rate of change of temperature of the slab. Since it is assumed that electrical energy is the only source of heat generation and there are no other losses, $\frac{dQ}{dt}$ can be set equal to the electric power applied to the slab, as shown in Eq. (6).

$$mC\frac{\Delta T}{dt} = RI^2 \tag{6}$$

Combining Eqs. (3), (4), and (6), and considering that electrical conductivity is the inverse of resistivity ($\sigma = \rho^{-1}$), results in Eq. (7).

$$mC\frac{\Delta T}{dt} = \rho^{-1}\left(\frac{L^2}{A^3}\right)|E|^2 \tag{7}$$

In Eq. (7), the dimensions and material properties (except for resistivity (ρ)) are measureable and do not significantly change with temperature. The resistivity, however, is highly dependent on the temperature of the material. Since the electric field is dependent only on the slab geometry and the applied voltage [61], the resistivity is a good candidate for updating based on measured values in developing an FE model that represents the experimental setup. The temperature increase is proportional to ρ^{-1} and the resistivity value would be updated based on Eqs. (8) and (9), using the measured temperature increase resulting from application of a specific voltage.

$$\frac{\Delta T}{dt} \propto \rho^{-1} \tag{8}$$

$$\frac{\left[\frac{\Delta T}{dt}\right]_{measured}}{\left[\frac{\Delta T}{dt}\right]_{trial}} = \frac{[\rho^{-1}]_{measured}}{[\rho^{-1}]_{trial}} \tag{9}$$

To enable running the simulation to obtain initial results for $\left[\frac{\Delta T}{dt}\right]_{trial}$, trial values of resistivity for a given slab temperature are needed. In this study, this trial resistivity was determined based on the resistivity of ECON samples measured at 22 ˚C and the measured generated current increase in ECON from 0 ˚C to 22 ˚C resulting from the applied voltage.

2.3.2 Model-updating Based on Measured Power Demand

For this method, electric power required by the ECON system can be calculated by the Joule heat generation equation:

$$P = \frac{V^2}{R} \tag{10}$$

where V is the applied voltage. Based on Eq. (10), the power drawn from the energy source is proportional to the inverse of resistance of the system, so the ECON layer resistivity can be updated using Eq. (11), which considers the measured power demand with the model estimate.

$$\frac{\rho_{measured}}{\rho_{trial}} = \frac{P_{estimated}}{P_{measured}} \tag{11}$$

While model-updating based on power demand would result in a model that is representative of the system in terms of required power, the temperature increase at the surface of the ECON layer should be checked to ensure that the model is also representative of system performance in terms of capability for melting snow and/or ice.

2.4 Electricity Use and Power Demand of ECON HPS

2.4.1 System Size

The total electricity use (kWh) and power demand (kW) of the system could be evaluated on either a per-event or a total winter season basis, assuming an ECON HPS constructed as described herein are implemented as the only snow and ice removal method for all typical snow and ice events at DSM. The concrete area where ECON could potentially be located includes the total apron area of DSM, approximately 139,400 m^2. Since it is unlikely that ECON HPS would be implemented to cover the total area of apron, the electricity use and power demand are calculated based on sizes of four different gate types, to provide a per-gate evaluation. This calculation assumed that 100% of a gate area would be equipped with ECON HPS, as a worst-case scenario, however a smaller portion of the gate area could also feasibly be considered. The approximate required area of apron for each gate type is 2,400 m^2 for Type A, 2,600 m^2 for Type B, 3,000 m^2 for Type C, and 6,500 m^2 for Type D [62]. DSM includes a total of 12 gates, and it is likely that airport managers would want to keep some, if not all, of the gates in operation under winter weather conditions either while it is snowing or after a snowfall. Therefore, providing the results on a per-gate basis can provide decision makers with improved capability for prioritizing ECON HPS operations with respect to highly-used or high-priority gates.

2.4.2 Typical Weather Conditions at DSM

The weather data used to determine the number of snow events and the amount of snow was the Typical Meteorological Year (TMY2) [63] dataset, developed to represent typical conditions in a particular location of interest. TMY3 or TMY4 are not used since snow

thickness values are not included in these data sets. TMY2 is based on approximately 20 years of historical weather data for the location of DSM, with data provided in hourly increments. Typical snow events were extracted from this data using daily snow thickness, ambient temperature, and wind speed values. The daily snow thickness is translated to a uniform snowfall rate for the duration of the day when the ambient temperature was below 0°C. Considering a density of 100 kg/m^3 for the snow [64], a heat flux has been calculated for the snowfall rate using the latent heat required to melt the ice form of water [64]. For each snow or ice event, the temperature, wind speed, and snowfall rate are applied to the model to calculate the power demand of the system to melt the snow. Since the wind speed data available in the TMY dataset are for a height of 10 m above ground level, from those values, wind speed values at 0.5 m above ground level were calculated based on the methodology presented by Qin and Hiller [65] and Sadati et al. [66]. Using this method the wind speed w_1 at height h_1 is related to the wind speed w_2 at a height h_2 using Eq. (12). Wind speed is in (m/s) and height is in (m).

$$\frac{\mathrm{W}_1}{W_2} = \left(\frac{h_1}{h_2}\right)^{1/7} \tag{12}$$

2.4.3 Electricity Use and System Control Strategy

To determine the electricity use (kWh) of the total duration of heating, the associated electricity demand profiles are added together at hourly time steps to determine the final electricity use. To determine the average electricity use on a per-event basis, the total electricity use is divided by the number of unique snow or ice events that occurred over the 1 year period of evaluation. Based on the experience of the research team in testing the test slabs of ECON HPS at DSM, since the date of a snow event can be predicted with a higher accuracy than the

exact time of snowfall during that day, it is assumed that the ECON HPS would operate for the entire 24 hours of the day of a predicted snow event. This assumption is made to simplify the evaluation of electricity use of the ECON HPS, since "typical" hourly snow thickness data are not available. Under actual field conditions, based on experimental data, the system could be turned on several hours before onset of predicted snow, such that when snowfall begins the surface temperature would be above the freezing point to prevent snow accumulation. To this end, the control system is given a setpoint as the desired surface temperature and the ECON HPS will automatically turn on whenever the temperature falls below this setpoint. The setpoint in this study is assumed to be 5 ˚C which guarantees that temperature of all locations on the surface is above freezing point (0 ˚C). The temperature of the surface is checked every half hour since based on initial results the temperature is not expected to go below freezing point in half an hour considering that the sublayers and bottom of the ECON layer also have higher temperatures.

CHAPTER 3. RESULTS AND DISCUSSIONS

The methodology introduced in Section 2 is applied and the results for ECON HPS performance in terms of electricity use and ability to melt ice and snow in typical climatic conditions of DSM are reported and discussed in this section. These subsections include the results of the model-updating based on temperature measurements and power demand and the performance of the system under the conditions of typical snow events at DSM.

3.1 Model of a Laboratory Test Slab

To estimate the performance of the system before building the actual experimental setup at DSM and to determine the best locations for placing the sensors, a FE model of the laboratory test slab was built in ANSYS 18.2 [57] as shown in Figure 5. Since all sides of the slab other than the surface were isolated, it was assumed that heat transfer is negligible from all sides except the slab's surface. A convection load was applied to the surface of the ECON layer to account for the heat loss from the surface to the ambient air with which it interfaces. Material properties including electric resistivity, heat capacity and thermal conductivity were considered for this analysis. Weather conditions applied to the model included ambient air temperature and wind speed. The shape and configuration of the FE elements of the developed model are shown in Figure 5.

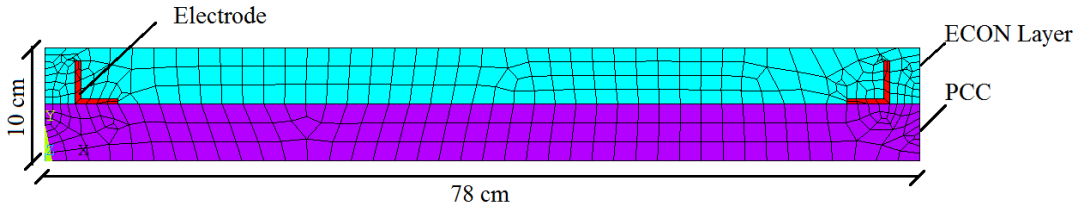

Figure 5. Elements of the finite element model of the ECON laboratory test slab.

A transient solution method was utilized to determine the temperature increase trend over time. The time step used for this solution was 5 minutes, which was the time step of recording the measured temperatures.

The temperature distribution resulting from FE model of the laboratory test slab is compared with the experimental temperature increase at the middle of ECON layer. Figure 6 illustrates the temperature distribution in both ECON and PCC layers from the model results. As shown in the Figure, the temperature is warmer at the middle of the slab and there is no heat concentration on the electrodes and the temperature distribution over the surface is uniform.

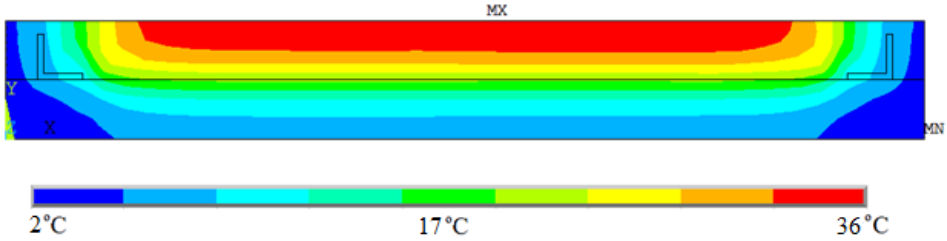

Figure 6. Temperature distribution resulted from the finite element model

The electric resistivity of the ECON measured at 28 days curing time and the weather conditions during that day were applied to the model to compare the measured temperature of the ECON layer with model predictions during its operation. As shown in Figure 7, the increasing trend of measured temperature for the center point of the ECON layer generally matches the temperatures predicted by the model within +/- 20%.

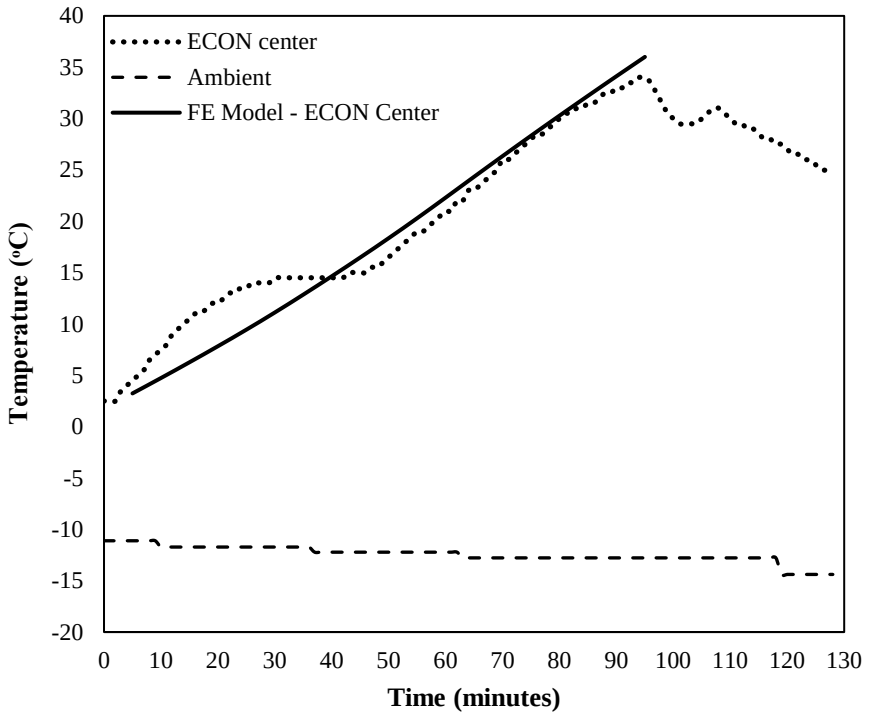

Figure 7. Temperature increase at the center of ECON layer measured on 28th day of construction and predicted by the model; *Note: at 95 minutes the system was turned off, thus the observed drop in ECON temperatures*

3.2 Measured Temperature and Electric Current Values for DSM Test Slabs

Measured values of electric current and temperature in different layers of pavement system are shown in Figure 8 through Figure 10, for test events on the 24 and 27 of December. 2017, respectively. There are some missing values for one of the sensors located 3.5 inch from the pavement surface. This is due to the existence of electric current in ECON layer which interferes with sensor readings.

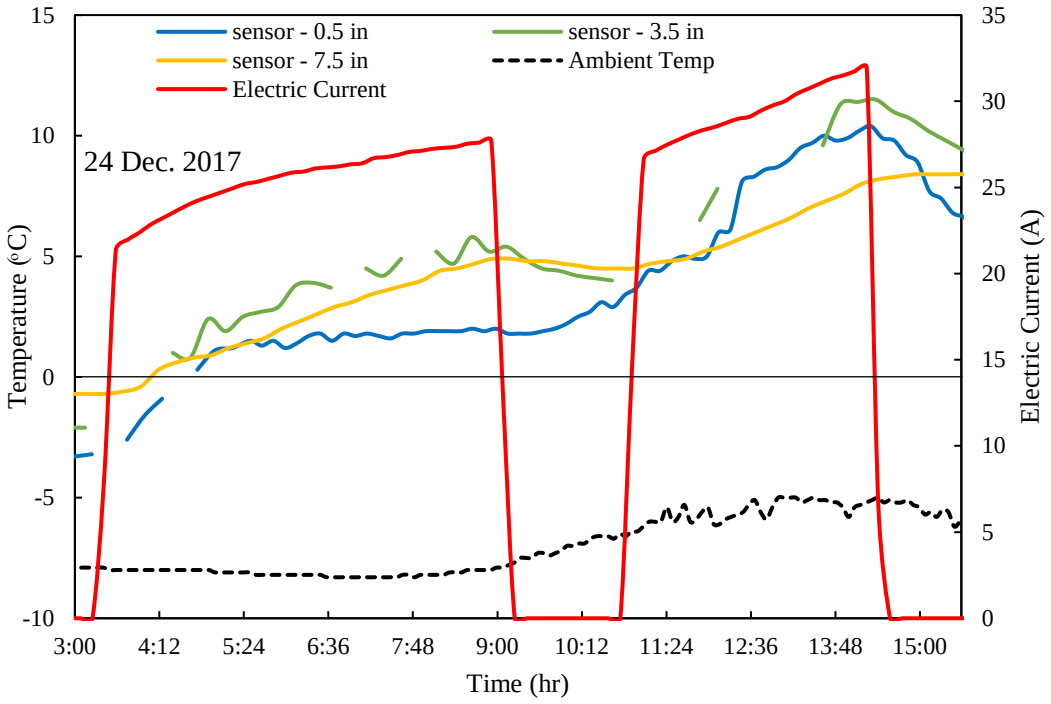

Figure 8. Electric current and temperature variations in different layers of the pavement on 24 December 2017

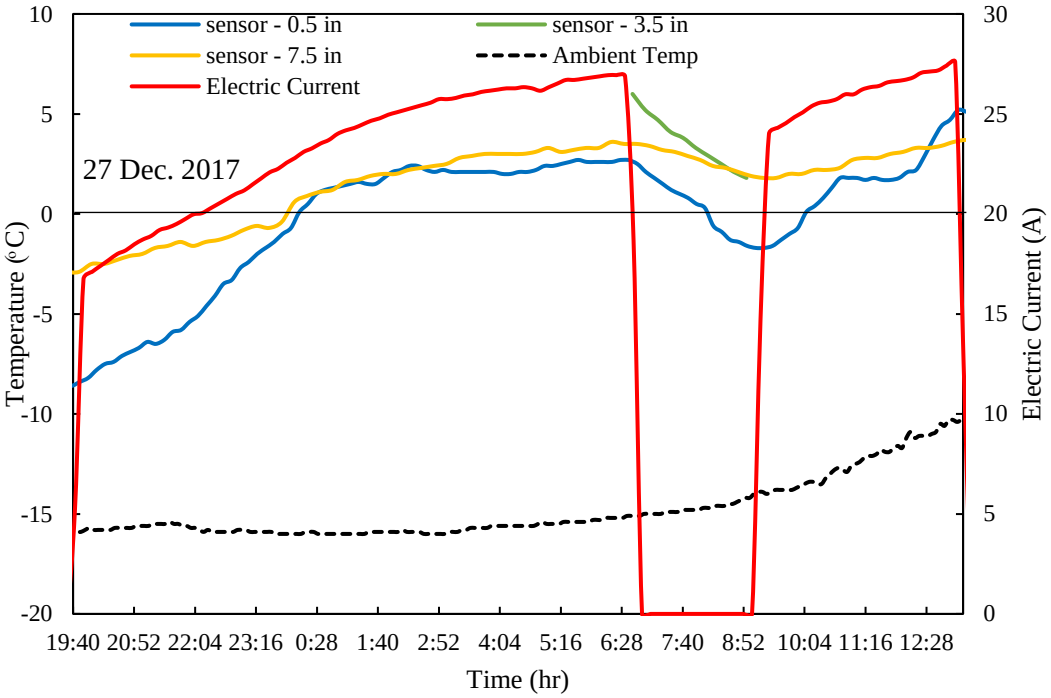

Figure 9. Electric current and temperature variations in different layers of pavement and ambient temperature on 27 December 2017

As shown in Figure 8 and Figure 10, as soon as the system is turned on, the electric current value increases followed by a continuous increase in pavement temperature values. The temperature of the deeper pavement layers are initially higher than the temperature of surface layers. Since the heat loss from the surface of the pavement is the largest the closest sensors to the surface usually show the lowest temperatures, unless the system is turned on. The thickness of ECON layer is 3.5 inch and electrodes are placed at the bottom of this layer. Therefore, the bottom of ECON layer heats faster and the sensor at 3.5 inch shows the highest temperature between all sensors. As soon as the system is turned off (i.e. the electric current value drops to zero), the pavement temperature begins decreasing which happens faster at the surface unless existence of solar radiation heats the surface.

3.3 Model-updating Based on Average Temperature

The data from Experimental Test 1 which occurred on 10 December 2016 (Table 2), including weather conditions and measured temperature and values, are used for the model-updating. The measured resistivity values are used as the trial resistivity values for the model. After model-updating based on the temperature values, the updated resistivity of the ECON layer is calculated. The trial resistivity and updated resistivity values are shown in Figure 10. As shown, the resistivity of ECON decreases with an increase in slab temperature, consistent with the behavior of the resistivity for concrete as reported in the literature [60]. Modifying the resistivity of the model to the updated resistivity values as shown in Figure 10, transient thermal analysis is conducted for a simulation time of 5.5 hours, the duration of Experimental Test 1 in the field.

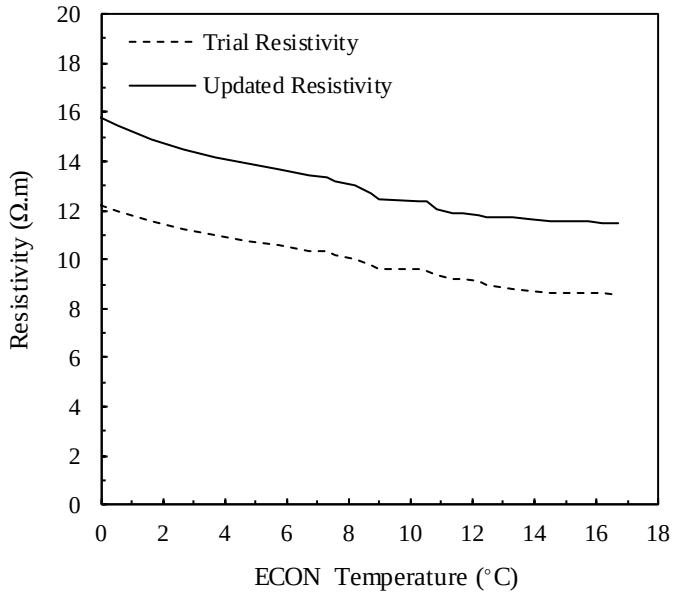

Figure 10. Electrical resistivity of ECON versus temperature for the FE model before and after model-updating by measured temperatures

Figure 11 illustrates the temperature distribution throughout the slab and the heat transfer both to the base layers and to the subgrade. Initial temperatures are assumed for different layers of the pavement based on temperature measurements from sensors embedded in different pavement layers. Since the model is axisymmetric there is no temperature gradient in the direction of the x axis. Although this model is axisymmetric, a 3D model is developed to provide capability in future studies for applying different boundary conditions from the different sides of the slab.

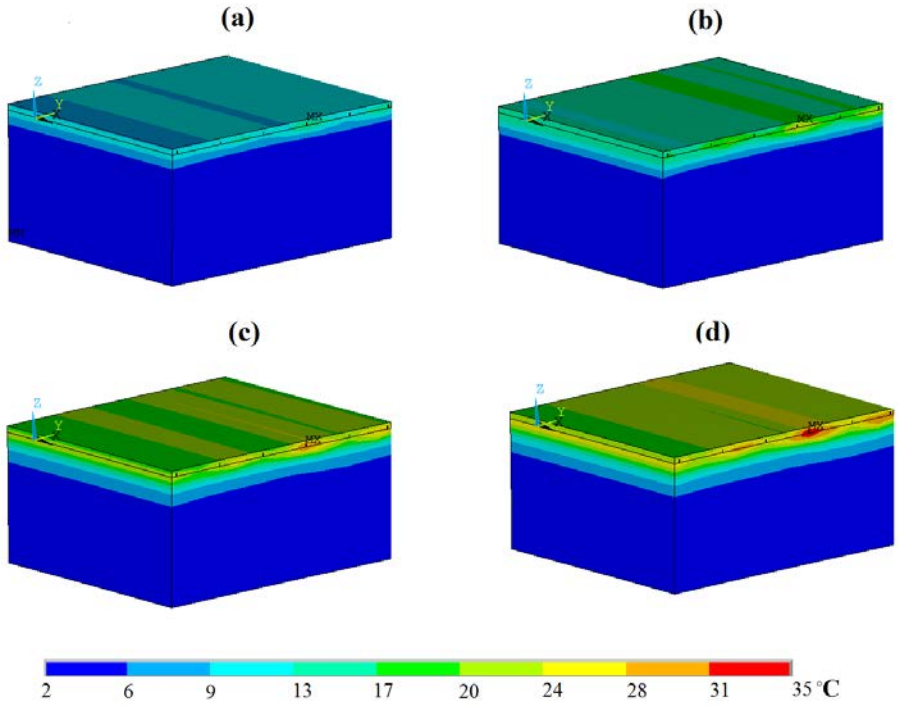

Figure 11. Temperature contours after (a) 1.4 hr, (b) 2.8 hr, (c) 4.2 hr, and (d) 5.5 hr of operation

Since in Experimental Test 1 the resistivity was updated using the average temperature of the ECON layer, for this test the average ECON layer temperature resulting from the model and measured in the field are compared in Figure 12. The measurement error bars shown in the figures are calculated based on the potential errors of each sensor. The average ECON layer temperature was measured using the thermistor sensors embedded in this layer. As shown, the FE model results for this test event are consistent with measured temperatures. Therefore, the promising performance potential of the introduced model-updating method can be observed by comparing the non-updated FE and the updated FE model results. The power demand of ECON HPS, both measured at the field and estimated by the updated model based on temperature of the slab, are shown in Figure 13. Although the model-updating method based on measured temperature values aims to improve the estimated thermal performance of the model, it can also improve the power demand estimation with a maximum error of 5%. This

updating method can therefore be used for accurately estimating thermal performance and can also provide a close estimation of the power demand.

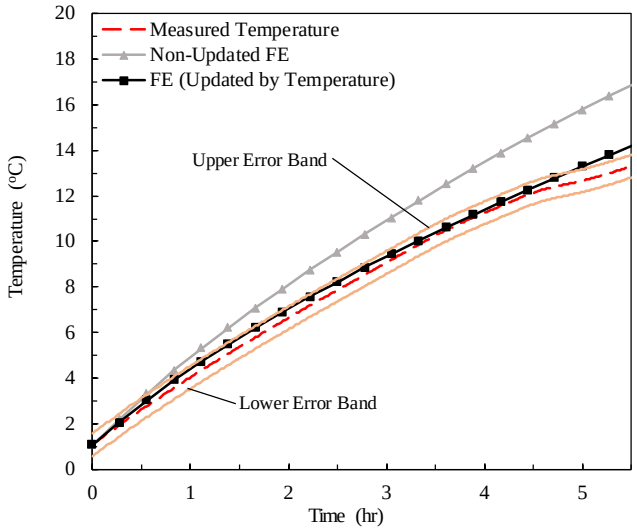

Figure 12. Average temperature of ECON layer for Experimental Test 1 including finite element model simulation results before and after model-updating using measured temperatures (*Note: the average ambient temperature across the test period is -5 ˚C and average wind speed measured at the height of 10 m is 5.8 m/s; upper and lower error bands present the potential error in measurement calculated using the error value of the temperature sensors)*

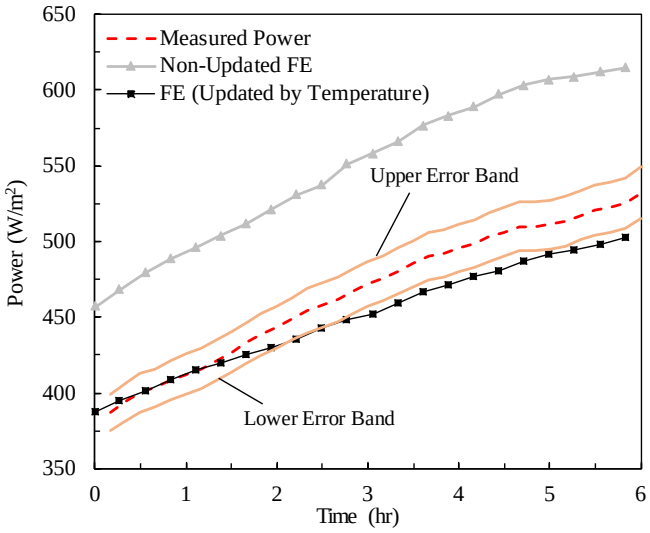

Figure 13. Measured and estimated electric power demand of the ECON HPS for Experimental Test 1 including finite element model simulation results before and after model-updating using measured temperatures *(Note: the average ambient temperature is -5 ˚C and average wind speed measured at the height of 10 m is 5.8 m/s during the test period; upper and lower error bands present the measurement error calculated using potential error values for voltage and electric current sensors.)*

To evaluate the performance of the model in weather conditions varying from those used for updating the model, Experimental Test 2 weather and performance, on 9 December 2016, data (Table 2) are considered. Figure 14 illustrates the average temperature increase of the ECON layer for Experimental Test 2, reflecting consistency with the measured values and indicating that the model is performing well under different weather conditions and for out-of-sample data.

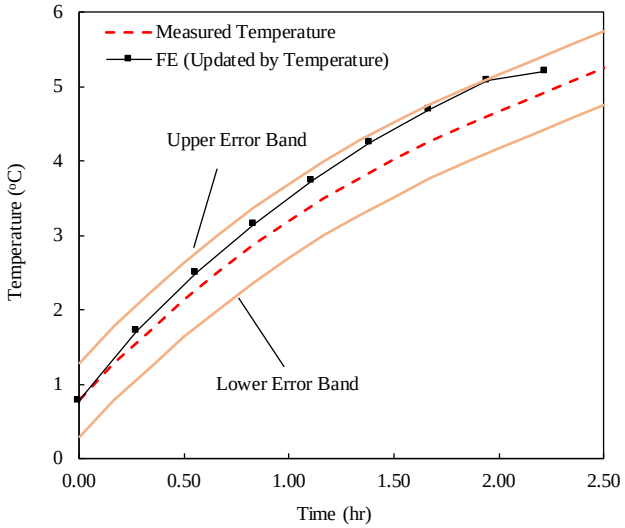

Figure 14. Average temperature of ECON HPS test slab for Experimental Test 2 including finite element model simulation after model-updating using measured temperatures (*Note: the average ambient temperature is -10 ˚C and average wind speed measured at the height of 10 m is 10 m/s; upper and lower error bands present the potential error in measurement calculated using the error value of the temperature sensors)*

3.4 Model-updating Based on Power Demand

The trial and updated resistivity values obtained by applying model-updating based on power demand and using Experimental Test 1 data are shown in Figure 15. The updated resistivity based on power demand is 16.7% less than the updated resistivity based on the slab temperature and is closer to the measured resistivity (trial resistivity). Measured power and estimated power demand before and after model-updating are shown in Figure 16. The lower

resistivity value results in the system's capability for drawing more power from the source. Therefore, while the increase in temperature after updating by power demand (Figure 17) is greater than the increase in the temperature after updating by average temperature (Figure 12), the temperature estimation improves after applying the updating method, so updating the model by power demand would result in more accurate estimation of the electricity use of the system and the estimation of thermal performance.

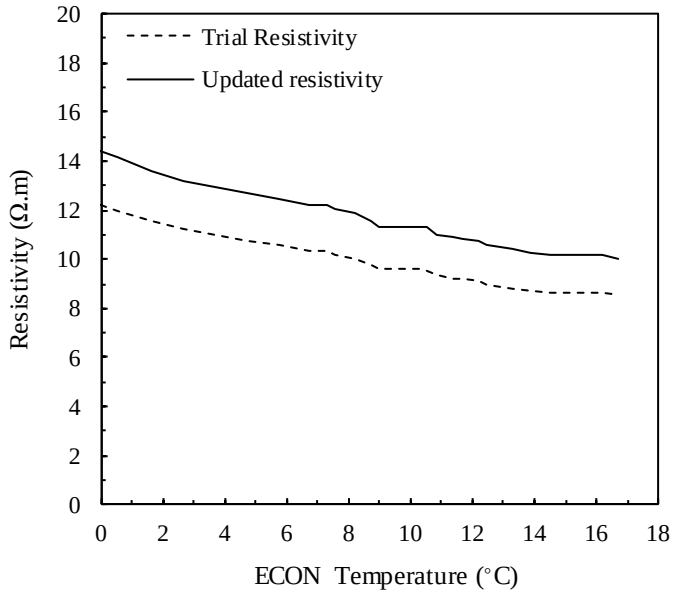

Figure 15. Electrical resistivity of ECON versus its temperature before and after model-updating using measured power demand of ECON HPS

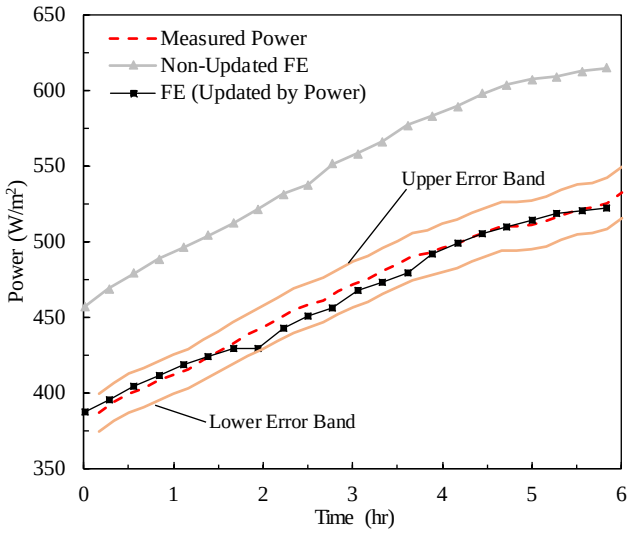

Figure 16. Measured and estimated electric power demand of the ECON HPS for Experimental Test 1 before and after model-updating using measured power demand of ECON HPS (*Note: the average ambient temperature is -5 ˚C and average wind speed measured at the height of 10 m is 5.8 m/s during the test period; upper and lower error bands present the measurement error calculated using potential error values for voltage and electric current sensors)*

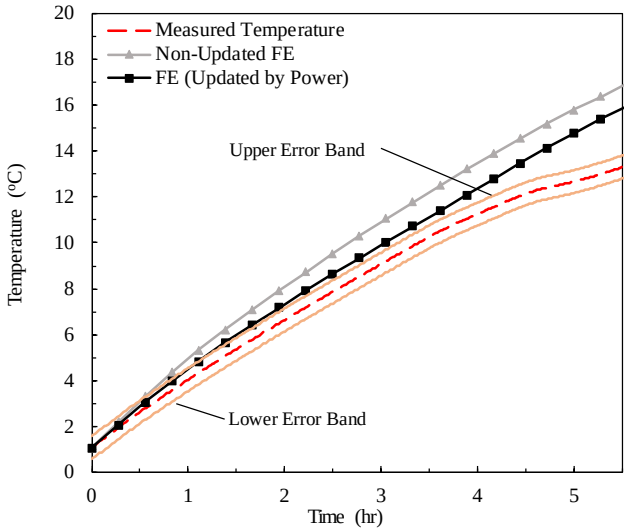

Figure 17. Average temperature of ECON layer for Experimental Test 1 including finite element model simulation results before and after updating using measured power demand of ECON HPS *(Note: the average ambient temperature is -5 ˚C and average wind speed measured at the height of 10 m is 5.8 m/s during the test period; upper and lower error bands present the potential error in measurement calculated using the error value of the temperature sensors)*

The weather conditions for Experimental Test 2 are applied to the FE model updated by power demand measured for Experimental Test 1 and the estimated electric power demand

is shown in Figure 18. As shown, the estimated power demand is very close to measured values and this model updated by power is used to evaluate the performance of the system.

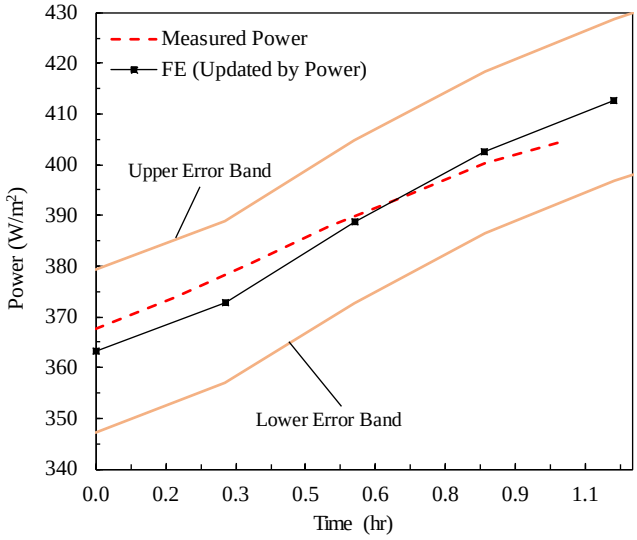

Figure 18. Electric power demand of ECON HPS for Experimental Test 2, including model results after updating using measured power demand of the slab, compared to measured data (*Note: the average ambient temperature is -10 ˚C and average wind speed measured at the height of 10 m is 10 m/s during the test period; upper and lower error bands present the measurement error calculated using potential error values for voltage and electric current sensors)*

3.5 Evaluation of Electricity Use of ECON system

3.5.1 ECON HPS Performance during Typical Snow Events at DSM

The electricity use of the system under typical snow events at DSM can be evaluated based on the model updated by power demand. Hourly ambient temperature, hourly wind speed, and daily snow thickness values were obtained for 32 identified snow events for DSM using the TMY data. These values were applied to the model and the power demand was calculated for each snow event.

Two examples of winter climatic conditions, snow event A and snow event B, representing two sample snow events, have been selected for discussion herein. Snow event A

has been selected as an event that the system successfully increases the surface temperature above the setpoint (5 ˚C) and maintains it. Snow event B is the only event in which the surface temperature is increased to the setpoint, but the system fails to maintain that temperature because of the extreme cold weather conditions. Ambient temperature and wind speed are shown in Figure 19 and average temperature of the slab surface is shown in Figure 20 for snow event A. The system turns off and on frequently after it reaches the setpoint temperature so as not to increase the temperature to more than the setpoint value.

Ambient temperature and wind speed values for snow event B are shown in Figure 21. The average temperature of the surface in this case is shown in Figure 22. As can be seen, in extremely cold and windy weather conditions the system was not able to maintain the setpoint temperature for all hours because of high heat loss from the surface of the slab. Out of the 32 typical snow events, however, this is the only one where the designed system is unable to maintain an average surface temperature above the freezing point. In future studies the limitations of the system should be further investigated for these and other extreme weather conditions.

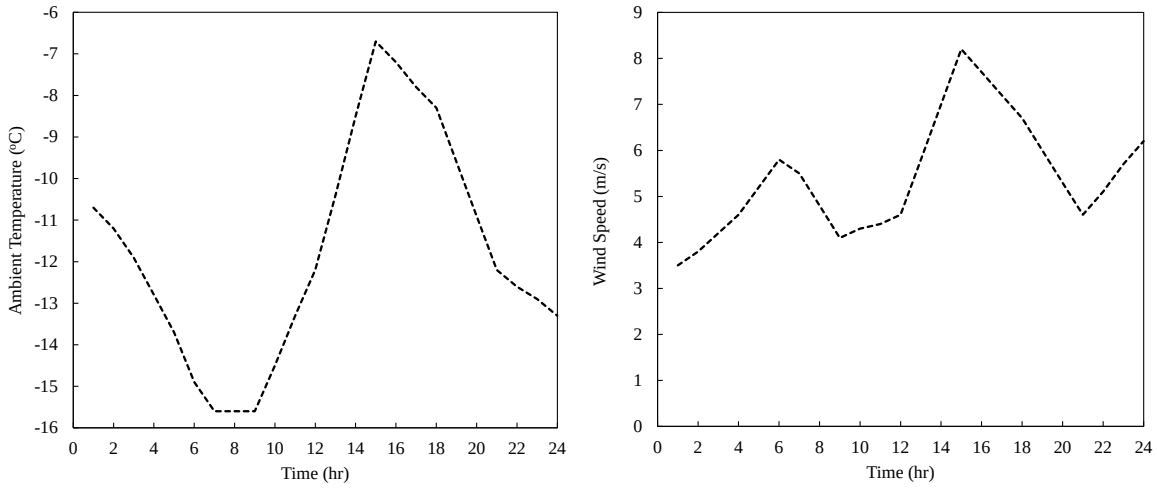

Figure 19. Ambient temperature and wind speed obtained from TMY (typical meteorological year) data for typical snow event A

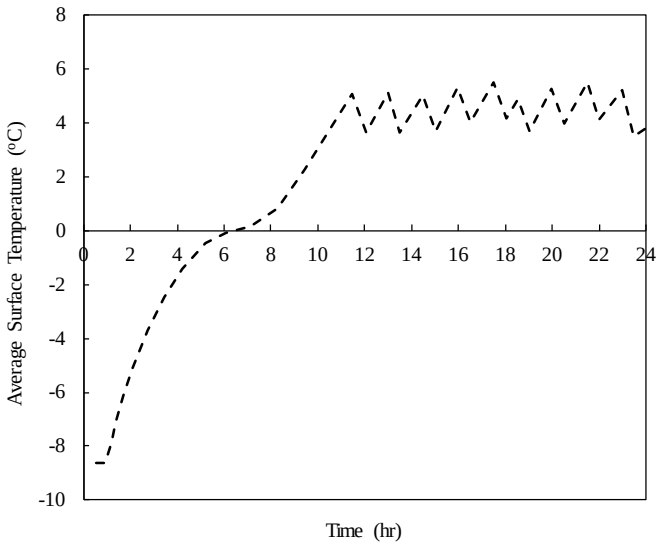

Figure 20. Estimated average surface temperature for ECON HPS for typical snow event A

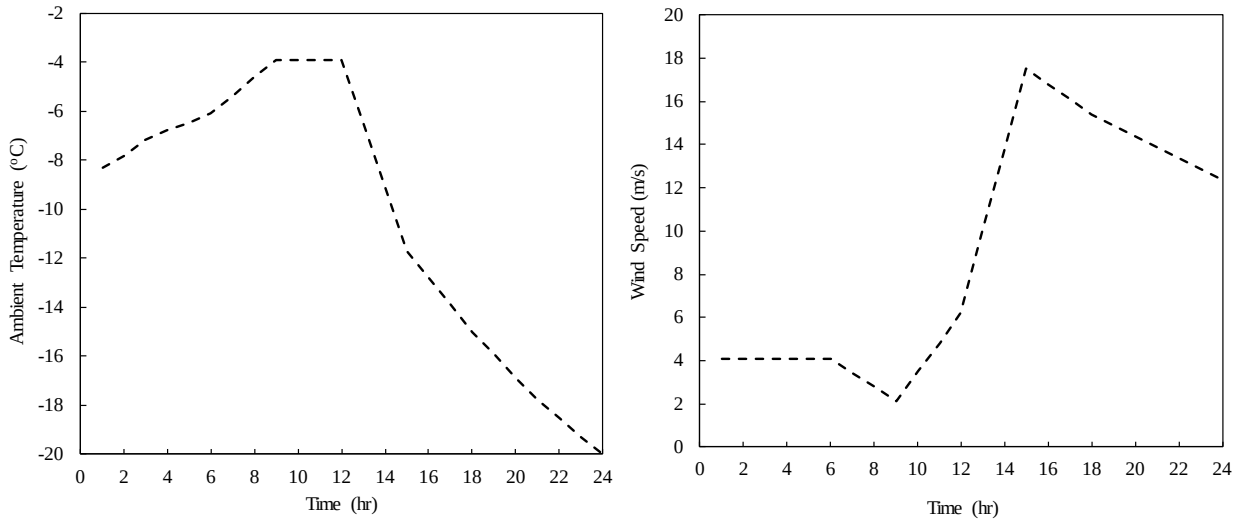

Figure 21. Ambient temperature and wind speed obtained from TMY (typical meteorological year) data for typical snow event B

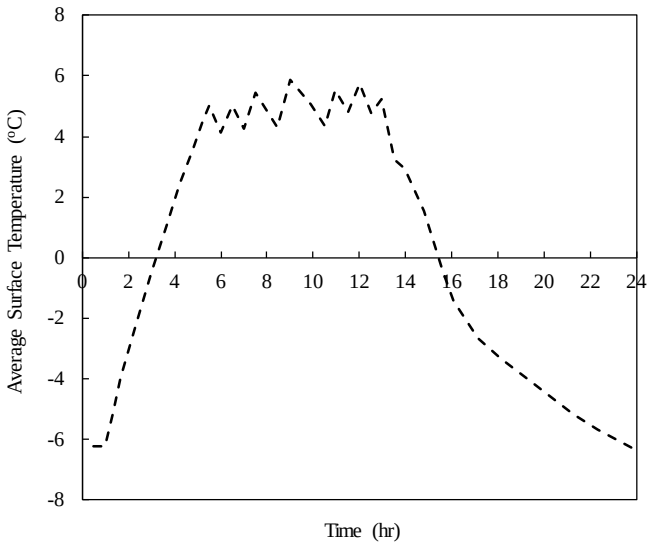

Figure 22. Estimated average surface temperature for ECON HPS for typical snow event B

3.5.2 Power Demand and Electricity Use for ECON HPS

To calculate the power demand, it is assumed that the ECON HPS will be implemented in the gate areas for each gate type introduced in subsection 2.4.1. The power demand is calculated by running the model using inputs representing the 32 typical snow events. The power demand for the two typical snow events discussed in subsection 3.5.1 are shown in Figure 23. Due to the higher heat loss from the slab surface in event B which results in lower ECON temperature and higher ECON resistivity, more energy is required if the system is to be able to maintain the setpoint temperature. These higher energy requirements would be provided by decreasing the resistivity of ECON layer and keeping the same applied voltage level. The minimum input energy rate for a hydronic system is reported to be 400 W/m^2 in [36] which is consistent with the values obtained for ECON HPS.

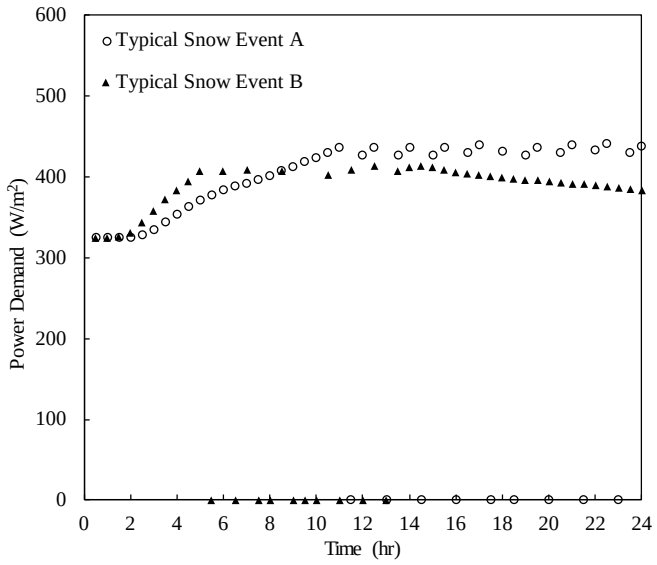

Figure 23. Estimated power demand of the ECON HPS for typical snow events A and B; Note: data points for power demand are shown at 30 minute intervals; power demand is zero when the system is turned off so as not to overheat the slab surface

Considering all the 32 typical events and using power demand calculations from the FE model, the electricity use is calculated for each gate type. The monthly electricity use of the system for these gate types for each month of the winter is calculated and compared to the corresponding use at DSM Terminal, a three-story building with 12 gates and an area of approximately 7,000 m^2, as shown in Figure 24. The ECON layer resistivity is the driving factor for the electricity use of the ECON HPS. Laboratory samples of ECON material exhibited resistivity values approximately ten times lower than those of the ECON material used in the field at DSM. The reason for this difference is the higher efficiency of the mixing procedure in the lab compared to the larger-scale mixing used in the field. It is therefore possible to improve the efficiency of ECON HPS by improving the larger-scale mixing procedure.

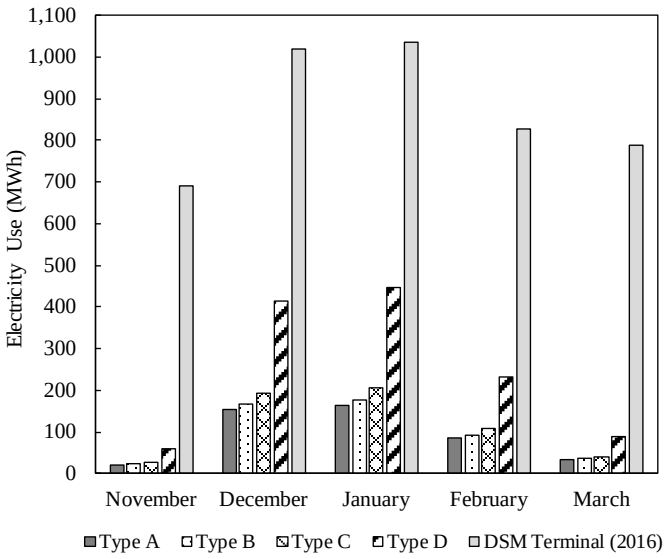

Figure 24. Estimated monthly electricity use of ECON HPS per gate size for each gate type, considering typical snow events from TMY data in Des Moines, Iowa, in comparison to the measured total monthly electricity use of the DSM Terminal in 2016

An ECON HPS provides the greatest potential benefit and use for pavements located in cold climate regions, because snow and ice removal is an essential process in these locations. However, even in mixed climate regions that also experience intermittent snow and ice conditions in the winter, critical airport operations may also require substantial snow and ice removal equipment and associated operational budgets [14]. As reported by Anand, et al., [14], in airports with more than 40,000 annual flight operations, critical airport areas should be cleared of snow and ice within a half hour after one inch of snowfall. Satisfying this criteria requires availability of equipment and personnel with an associated high cost of operation, thus mixed climates' airports can also benefit from ECON HPS.

CHAPTER 4. CONCLUSIONS AND FUTURE WORK

A FE model was developed in ANSYS to simulate the performance of ECON HPS test slabs constructed at DSM connected to a 210 V power source, to evaluate the long-term energy demands of this large-scale system. The FE model consisted of all layers of the pavement, including the ECON, PCC, base, and subgrade layers. Methodologies for FE model updating based on measured electric power demand and temperature data were developed and presented, and the resistivity of the model was updated in order to improve the model results. Updating based on power demand was found to provide more accurate estimation of energy consumption, thus it was used for evaluation of system performance under typical weather conditions for snow events at DSM. The model was programmed to run for all hours of each snow event day, increase the average surface temperature to a setpoint (5 ˚C) and maintain this temperature while the system was in operation. Energy consumption for four different sizes of airport gates was compared to the overall usage of the DSM Terminal. Among 32 typical snow events, in only one case was the system estimated to be unable to keep the surface temperature at the given setpoint due to a low minimum ambient temperature of -24 ˚C and a high maximum wind speed of 18 m/s. In summary, the major findings of this study include the following:

- The developed model-updating methods work effectively to improve both temperature and energy use predictions of ECON HPS.
- Energy and thermal performance of ECON HPS highly depend on the weather conditions (ambient temperature, wind speed and snowfall rate), therefore, it is recommended to study the performance of the designed system using a broad range typical weather conditions as input.

- Electric power demand of the designed ECON HPS at DSM is about 325 to 460 W/m^2 depending on the weather conditions.
- The economic feasibility of implementing ECON HPS would be impacted by its power demands considering the demand charge-based billing system of utility companies typically employed for commercial installations.
- The control strategy of operating ECON HPS affects the overall power demand and electricity use of the system. This control strategy should be further studied to optimize the power demand while ensuring the thermal performance is adequate enough to facilitate modulating the temperature of pavement to melt snow and ice.
- ECON layer resistivity is the main driving factor for energy consumption; improving the large-scale concrete mix techniques could result in energy savings by increasing overall system efficiency.

4.1 Limitations of this work

Since hourly typical snowfall data were not available, the analysis was conducted based on daily values of snow thickness, even though having data with a higher time resolution would result in more precise modeling. The results are also limited to the weather conditions In addition, although the material properties needed for modeling were measured for ECON, these data were obtained from literature for other pavement layers. The accuracy of the analysis could be improved having the measured material properties of pavement sublayers. Therefore one of the main limitations of this study is the material properties and design configuration of the investigated case.

4.2 Future Work

In future studies different control strategies for reducing the power demand, such as by varying the voltage while the system is running, should be investigated. Operating the system intermittently could also result in reducing the overall power demand. This control strategy would be based on dividing the total surface of ECON HPS into several zones and turning each zone on/off in cycles. The frequency of this cyclic operation of the defined zones would be a significant parameter to be studied. Moreover, the potential for implementing ECON HPS in residential areas and utilizing renewable energy resources for powering ECON HPS should be studied. These topics are discussed briefly in the following subsections.

4.2.1 Potential Use of ECON HPS for Residential Sectors

Although this research focused on the application of ECON HPS for airports apron area, this technology could also be used for residential building sector applications as well. These comparisons between the electricity use of ECON HPD and the DSM terminal building (Figure 24) show the potential for the utilization of ECON HPS in the residential building sector, since its power demand is comparable with the power demand intensities of current building technologies. Nevertheless, reducing the power demand of buildings is currently a focus area of building performance studies and there is much research suggesting the necessity of reducing the power demand of buildings for improved sustainability [67,68]. These studies alert us to the increasing power demands associated with residential buildings. Since implementing ECON HPS would eventually result in an additional increase in power demand, it is important to study the necessity of the application of ECON HPS for the residential sector by comparing its performance with other snow/ice removal techniques.

4.2.2 Use of Renewable Energy Sources to Power ECON HPS

The increasing trend of electricity use in all residential, commercial and industrial sectors is estimated to be problematic in the future since the majority of resources used to generate electricity are fossil fuel-based. Fossil fuel resources are associated with two main challenges: *i*) negative environmental impacts due to the emission of greenhouse gasses, and *ii*) limited availability of resources [66,69]. Renewable resources are currently considered as a feasible alternative to fossil fuel-based resources [70]. Therefore, the potential for utilizing renewable energy resources for powering ECON HPS should also be studied in further detail. ECON HPS is a technology best suited for regions with considerable snowfall frequencies and cold winters, hence, the availability of renewable resources in those regions should be investigated further.

REFERENCES

[1] ACRP, 2008, *Airport Sustainability Practices*.

[2] Kilkiş, B., and Kilkiş, Ş., 2016, "New Exergy Metrics for Energy, Environment, and Economy Nexus and Optimum Design Model for Nearly-Zero Exergy Airport (nZEXAP) Systems," Energy, **140**, pp. 1–21.

[3] Uysal, M. P., 2017, "An Integrated Research for Architecture-Based Energy Management in Sustainable Airports," Energy, **140**, pp. 1387–1397.

[4] Roskilly, A. P., Palacin, R., and Yan, J., 2015, "Novel Technologies and Strategies for Clean Transport Systems," Appl. Energy, **157**, pp. 563–566.

[5] Gopalakrishnan, K., Ceylan, H., Kim, S., Yang, S., and Abdualla, H., 2015, "Self-Heating Electrically Conductive Concrete for Pavement Deicing: A Revisit," *Transportation Research Board 94th Annual Meeting.*, p. No. 15-4764.

[6] Ramakrishna, D. M., and Viraraghavan, T., 2005, "Environmental Impact of Chemical Deicers--a Review," Water. Air. Soil Pollut., **166**(1–4), pp. 49–63.

[7] Quilty, S. M., 2015, *Airside Snow Removal Practices for Small Airports with Limited Budgets*.

[8] ACRP, 2013, *Apron Planning and Design Guidebook*, Transportation Research Board, Washington, D.C.

[9] Shen, W., 2015, "Life Cycle Assessment of Heated Airfield Pavement System for Snow Removal," Graduate Thesis and Dessertation, Iowa State University.

[10] Anand, P., Ceylan, H., Gkritza, K. N., Taylor, P. C., Pyrialakou, V. D., Kim, S., and Gopalakrishnan, K., 2014, "Establishing Parameters for Cost Comparison of Alternative Airfield Snow Removal Methodologies," The 2014 FAA Worldwide Airport Technology Transfer Conference, August 5-7, 2014, Galloway, New Jersey.

[11] Suraneni, P., Azad, V. J., Isgor, O. B., and Weiss, W. J., 2016, "Deicing Salts and Durability of Concrete Pavements and Joints," Concr. Int., **38**(4), pp. 48–54.

[12] Amini, B., and Tehrani, S. S., 2014, "Simultaneous Effects of Salted Water and Water Flow on Asphalt Concrete Pavement Deterioration under Freeze-Thaw Cycles," Int. J. Pavement Eng., **15**(5), pp. 383–391.

[13] Casey, P. C., Alwan, C. W., Kline, C. F., Landgraf, G. K., and Linsenmayer, K. R., 2014, *Impacts of Using Salt and Salt Brine for Roadway Deicing*.

[14] Anand, P., Ceylan, H., Gkritza, K., Talor, P., and Pyrialakou, V. D., 2014, "Cost Comparison of Alternative Airfield Snow Removal Methodologies."

[15] Won, J. P., Kim, C. K., Lee, S. J., Lee, J. H., and Kim, R. W., 2014, "Thermal Characteristics of a Conductive Cement-Based Composite for a Snow-Melting Heated Pavement System," Compos. Struct., **118**(1), pp. 106–111.

[16] Pan, P., Wu, S., Xiao, F., Pang, L., and Xiao, Y., 2014, "Conductive Asphalt Concrete: A Review on Structure Design, Performance, and Practical Applications," J. Intell. Mater. Syst. Struct., **26**(7), pp. 755–769.

[17] Pan, P., Wu, S., Xiao, Y., and Liu, G., 2015, "A Review on Hydronic Asphalt Pavement for Energy Harvesting and Snow Melting," Renew. Sustain. Energy Rev., **48**, pp. 624–634.

[18] Mensah, K., and Choi, J. M., 2015, "Review of Technologies for Snow Melting Systems," J. Mech. Sci. Technol., **29**(12), pp. 5507–5521.

[19] Hockersmith, S. L., 2002, "Experimental and Computational Investigation of Snow Melting on Heated Horizontal Surfaces," Oklahoma State University.
[20] Moon, C. E., and Choi, J. M., 2015, "Heating Performance Characteristics of the Ground Source Heat Pump System with Energy-Piles and Energy-Slabs," Energy, **81**, pp. 27–32.
[21] Liu, X., Rees, S. J., and Spitler, J. D., 2007, "Modeling Snow Melting on Heated Pavement Surfaces - Part II: Experimental Validation," Appl. Therm. Eng., **27**(5–6), pp. 1125–1131.
[22] Sadati, S. M. S., Cetin, K., and Ceylan, H., 2017, "Numerical Modeling of Electrically Conductive Pavement Systems," ASCE, Duluth, MN, pp. 1–10.
[23] Ceylan, H., Gopalakrishnan, K., Kim, S., and Cord, W., 2014, "Heated Transportation Infrastructure Systems: Existing and Emerging Technologies," The 12th International Symposium on Concrete Roads, September 23-26, 2014, Prague, Czech Republic.
[24] Tuan, C. Y., 2004, *Concrete Technology Today: Conductive Concrete for Bridge Deck Deicing*, Nebraska Department of Roads.
[25] Abdualla, H., Gopalakrishnan, K., Ceylan, H., Kim, S., Mina, M., Taylor, P., and Cetin, K. S., 2017, "Development of a Finite Element Model for Electrically Conductive Concrete Heated Pavements," the 96th Annual meeting of Transportation Research Board, January 8-12, 2017, Washington, D.C., pp. 1–18.
[26] Joskow, P. L., and Wolfram, C. D., 2012, "Dynamic Pricing of Electricity," Am. Econ. Rev., **102**(3), pp. 381–385.
[27] Gu, C., Yan, X., Yan, Z., and Li, F., 2017, "Dynamic Pricing for Responsive Demand to Increase Distribution Network Efficiency," Appl. Energy, **205**(July), pp. 236–243.
[28] Thelandersson, B. S., 1987, "Modelling of Combined Thermal and Mechanical Action in Concrete," **113**(6), pp. 893–906.
[29] Huang, Z., Platten, A., and Roberts, J., 1996, "Non-Linear Finite Element Model to Predict Temperature Histories within Reinforced Concrete in Fires," **31**(2).
[30] Khan, M. I., 2002, "Factors a Ecting the Thermal Properties of Concrete and Applicability of Its Prediction Models," **37**, pp. 607–614.
[31] Campbell-Allen, D., and Thorne, C. P., 1963, "The Thermal Conductivity of Concrete," Mag. Concr. Res., **15**(43), pp. 39–48.
[32] Shin, K., Kim, S., Kim, J., and Chung, M., 2002, "Thermo-Physical Properties and Transient Heat Transfer of Concrete at Elevated Temperatures," **212**, pp. 233–241.
[33] Kodur, V. K. R., and Sultan, M. a., 2003, "Effect of Temperature on Thermal Properties of High-Strength Concrete," J. Mater. Civ. Eng., **15**(2), pp. 101–107.
[34] Ã, Z. Z., Braun, J. E., Zhong, Z., and Braun, J. E., 2007, "A Simple Method for Estimating Transient Heat Transfer in Slab-on-Ground Floors," **42**, pp. 1071–1080.
[35] Selvam, R. P., and Castro, M., 2010, "3D FEM Model to Improve the Heat Transfer in Concrete for Thermal Energy Storage in Solar Power Generation," ASME 4th International Conference on Ennergy Sustainability, Phoenix, Arizona, pp. 1–9.
[36] Xu, H., and Tan, Y., 2015, "Modeling and Operation Strategy of Pavement Snow Melting Systems Utilizing Low-Temperature Heating Fluids," Energy, **80**, pp. 666–676.
[37] Liu, X., Rees, S. J., and Spitler, J. D., 2007, "Modeling Snow Melting on Heated Pavement Surfaces. Part I: Model Development," Appl. Therm. Eng., **27**(5–6), pp. 1115–1124.

[38] Wu, J., Liu, J., and Yang, F., 2015, "Three-Phase Composite Conductive Concrete for Pavement Deicing," Constr. Build. Mater., **75**, pp. 129–135.
[39] Sassani, A., Ceylan, H., Kim, S., Gopalakrishnan, K., Arabzadeh, A., and Taylor, P. C., 2017, "Influence of Mix Design Variables on Engineering Properties of Carbon Fiber-Modified Electrically Conductive Concrete," Constr. Build. Mater., **152**, pp. 168–181.
[40] Sassani, A., Ceylan, H., Kim, S., Gopalakrishnan, K., Arabzadeh, A., and Taylor, P. C., 2017, "Factorial Study on Electrically Conductive Concrete Mix Design for Heated Pavement Systems," *Transportation Research Board 96th Annual Meeting*, Washington DC, pp. 17–05347.
[41] Abdulla, H., Ceylan, H., Kim, S., Gopalakrishnan, K., Taylor, P. C., and Turkan, Y., 2016, "System Requirements for Electrically Conductive Concrete Heated Pavements," Transp. Res. Rec. J. Transp. Res. Board, **No. 2569**, pp. 70–79.
[42] Gopalakrishnan, K., Ceylan, H., Kim, S., Yang, S., and Abdualla, H., 2015, "Electrically Conductive Mortar Characterization for Self-Heating Airfield Concrete Pavement Mix Design," Int. J. Pavement Res. Technol., **8**(5).
[43] Abdulla, H., Ceylan, H., Kim, S., Mina, M., Gopalakrishnan, K., Sassani, A., Taylor, P. C., and Cetin, K. S., "Configuration of Electrodes for Electrically Conductive Concrete Heated Pavement," *ASCE International Conference on Highway Pavements and Airfield Technology*,.
[44] Sassani, A., Ceylan, H., Kim, S., Gopalakrishnan, K., Arabzadeh, A., and Taylor, P. C., 2017, "Factorial Study on Electrically Conductive Concrete Mix Design for Heated Pavement Systems," *Transportation Research Board 96th Annual Meeting*, Washington DC, pp. 17–05347.
[45] FAA, 2014, *Advisory Circular 150/5370-10G: Standards for Specifying Construction of Airports*.
[46] FAA, 2005, "Advisory Circular 150/5370-17: Airside Use of Heated Pavement Systems," Area, (January), pp. 1–4.
[47] U.S. Department of Energy, and Northwest, P., 2013, "Building Science-Based Climate Maps," p. 2.
[48] Abdualla, H., Ceylan, H., Kim, S., Mina, M., Cetin, K. S., Taylor, P., Gopalakrishnan, K., Cetin, B., Yang, S., Sassani, A., and others, 2018, *Design and Construction of the First Full-Scale Electrically Conductive Concrete Heated Airport Pavement System at a US Airport*.
[49] Monnit, 2017, "Wireless Temperature Sensors" [Online]. Available: https://www.monnit.com/Products/Wireless-Sensors/Coin-Cell/Wireless-Temperature-Sensors. [Accessed: 22-Dec-2017].
[50] Geokon, 2017, "Vibrating Wire Strain Gage" [Online]. Available: http://www.geokon.com/4200-Series. [Accessed: 22-Dec-2017].
[51] Taylor, J., 1997, *Introduction to Error Analysis, the Study of Uncertainties in Physical Measurements*.
[52] National Oceeanic and Atmospheric Adminstration (NOAA), 2017, "National Centers For Environemental Information."
[53] National Renewable Energy Laboratory (NREL), 2017, "National Solar Radiation Data Base."
[54] Minessota Department of Transportation, 2007, "2007 Minessota DOT Pavement Design Manual," Minessota Dep. Transp., **0**(1), pp. 1–39.

[55] Deng, D., and Murakawa, H., 2006, "Numerical Simulation of Temperature Field and Residual Stress in Multi-Pass Welds in Stainless Steel Pipe and Comparison with Experimental Measurements," Comput. Mater. Sci., **37**(3), pp. 269–277.
[56] Burgan, B., and Baddoo, N., 2012, *Structural Design of Stainless Steel*.
[57] ANSYS Inc., 2018, "ANSYS®."
[58] 2012, *An Illustration of the Concepts of Verification and Validation in Computational Solid Mechanics*, ASME.
[59] Friswell, M., and Mottershead, J. E., 2013, *Finite Element Model Updating in Structural Dynamics*, Springer Science & Business Media.
[60] Gowers, K., and Millard, S., 1999, "Measurement of Concrete Resistivity for Assessment of Corrosion," ACI Mater. J., (96), pp. 536–541.
[61] Xixiang, Z., Benshan, Z., and Eyjolfsson, B., 1987, *Finite Element Resistivity Modelling Using Specialized Mesh Structure*, National Energy Authority, Reykjavik, Iceland.
[62] FAA, 1988, *Advisory Circular 150/5360-13: Planning and Design Guidelines for Airport Terminal Facilities*.
[63] National Renewable Energy Laboratory (NREL), 2000, "Typical Meteorological Year Data" [Online]. Available: http://rredc.nrel.gov/solar/old_data/nsrdb/1961-1990/tmy2/. [Accessed: 26-Dec-2017].
[64] Sihvola, A., and Tiuri, M., 1986, "Snow Fork for Field Determination of the Density and Wetness Profiles of a Snow Pack," IEEE Trans. Geosci. Remote Sens., (5), pp. 717–721.
[65] Qin, Y., and Hiller, J. E., 2013, "Ways of Formulating Wind Speed in Heat Convection Significantly Influencing Pavement Temperature Prediction," Heat Mass Transf. und Stoffuebertragung, **49**(5), pp. 745–752.
[66] Sadati, S. M. S., Qureshi, F. U., and Baker, D., 2015, "Energetic and Economic Performance Analyses of Photovoltaic, Parabolic Trough Collector and Wind Energy Systems for Multan, Pakistan," Renew. Sustain. Energy Rev., **47**, pp. 844–855.
[67] Cetin, K. S., 2015, "Smart Technology Enabled Residential Building Energy Use and Peak Load Reduction and Their Effects on Occupant Thermal Comfort," University of Texas at Austin.
[68] Cetin, K. S., and Novoselac, A., 2015, "Single and Multi-Family Residential Central All-Air HVAC System Operational Characteristics in Cooling-Dominated Climate," Energy Build., **96**, pp. 210–220.
[69] Evans, A., Strezov, V., and Evans, T. J., 2009, "Assessment of Sustainability Indicators for Renewable Energy Technologies," Renew. Sustain. Energy Rev., **13**(5), pp. 1082–1088.
[70] Sadati, S. M. S., Jahani, E., Taylan, O., and Baker, D. K., 2018, "Sizing of Photovoltaic-Wind-Battery Hybrid System for a Mediterranean Island Community Based on Estimated and Measured Meteorological Data," J. Sol. Energy Eng. Trans. ASME, **140**(1).